DOI: 10.32615/ps.2020.002 PHOTOSYNTHETICA 58 (SI): 443-451, 2020

Special issue in honour of Prof. Reto J. Strasser

Gradual changes in the photosynthetic apparatus triggered by nitrogen depletion during microalgae cultivation in photobioreactor

T.YU. PLYUSNINA[*,+], S.S. KHRUSCHEV[*], N.S. DEGTEREVA[*], I.V. KONYUKHOV[*], A.E. SOLOVCHENKO[**], M. KOUZMANOVA[***], V.N. GOLTSEV[***], G.YU. RIZNICHENKO[*], and A.B. RUBIN[*]

Department of Biophysics, Faculty of Biology, Lomonosov Moscow State University, Leninskie Gory 1/12, 119234 Moscow, Russia[*]
Department of Bioengineering, Faculty of Biology, Lomonosov Moscow State University, Leninskie Gory 1/12, 119234 Moscow, Russia[**]
Sofia University 'St. Kliment Ohridski', Department of Biophysics and Radiobiology, Faculty of Biology, 8 Dragan Tsankov Boulevard, 1164 Sofia, Bulgaria[***]

Abstract

Changes of photosynthetic activity during natural depletion of nitrogen in a batch culture of *Chlorella vulgaris* were studied using chlorophyll *a* fluorescence-based methods. Complex analysis including JIP-test, multiexponential approximation, and the analysis of differential curves was carried out on the recorded fluorescence transients. Three pivot points were detected in dynamics of the JIP-test parameters during culture growing. We associated these time points with different stages of mineral stress progress. Immediately after nitrogen exhaustion in the cultivation medium, a transient increase in the efficiency of PSII was detected. During this short period, the photosynthetic apparatus acclimated to the stress by reducing the number of PSII reaction centers, simultaneously increasing the effective cross section of the light-harvesting antenna per reaction center. However, prolonged nutrient starvation impaired the structure of the photosynthetic apparatus, deactivating the oxygen-evolving complex and impairing the overall electron transport.

Additional key words: chlorophyll fluorescence induction; continuous monitoring; Kautsky effect; OJIP curve.

Introduction

Photosynthetic organisms under natural conditions are constantly exposed to stress factors, such as drought, extreme temperatures, excessive irradiance, and depletion of mineral nutrients. To cope with the stress and return to normal functioning, the photosynthetic cell deploys the mechanisms of adaptation to the temporary adverse conditions. Understanding these mechanisms is a prerequisite for efficient management of natural and artificial ecosystems. Accordingly, this goal calls for fast and reliable methods for monitoring of the physiological conditions of plants and microalgae, their viability, and stress effects. Deteriorative effects of a stress can be either reversible or irreversible. In this regard, the early diagnosis of the onset of stress becomes increasingly important.

The analysis of chlorophyll *a* fluorescence transients (induction curves) is widely used in order to assess the activity of the photosynthetic apparatus (PSA) under various conditions, including stress factors (Strasser and Strasser 1995). Fluorescence transients are recorded non-invasively upon illumination of dark-adapted samples by a high-intensity light for a few seconds. The fluorescence intensity rises from an initial level F_0 to a maximum level F_m (at saturating light intensity) in less than a second and then falls again. The rising part of the fluorescence induction curve plotted on a logarithmic time scale includes several steps, or phases, commonly denoted by letters OJIP (Strasser and Strasser 1995). Additional phases (K and L) may be detected.

The appearance of the individual phases K, J, I, and P on the induction curve (OJIP curve) reflects the stages of electron transfer in PSII toward PSI end acceptors. Characteristics of the fluorescence rise phases (OJIP curve) reveal the efficiency of the initial stages of the photosynthetic electron transport. The OJ part of the curve

Received 15 September 2019, *accepted* 6 January 2020.
[+]Corresponding author; e-mail: plusn@yandex.ru
Abbreviations: A_{675} – A_{725} – chlorophyll content index (difference of optical densities measured at 675 and 725 nm); A_{725} – cell count index (optical density of the cell suspension measured at 725 nm); OEC – oxygen-evolving complex; PBR – photobioreactor; PSA – photosynthetic apparatus; RC – reaction center; SMEA – spectral multiexponential approximation.
Acknowledgements: Financial support of Russian Foundation for Basic Research (18-29-25050) is greatly appreciated.

is commonly called 'photochemical phase' (Stirbet *et al.* 2014), and it reflects the reduction of primary electron acceptors – pheophytin and the Q_A quinone. The JIP part of the curve, called 'thermal phase', reflects the reduction of mobile electron carriers; its parameters depend on temperature (Stirbet *et al.* 2014). When samples are heated, an additional phase (usually manifested as K-band) (Oukarroum *et al.* 2007) becomes detectable in the fluorescence transient as a local maximum at *ca.* 300 μs. K-band is related to the processes on the donor side of PSII. An increase of its magnitude indicates imbalance of the rate of photochemical charge separation in PSII RCs and the rate of electrons donation from the oxygen-evolving complex (OEC) to RC (Strasser 1997). It usually points to OEC inactivation **(**Strasser *et al.* 2004, Kalaji *et al.* 2014) but it may also be caused by an increase in light energy trapped by the antenna and delivered to PSII RC (Vredenberg 2008). Mineral starvation (Lin *et al.* 2009, Kalaji *et al.* 2014, Schmidt *et al.* 2016), water deficiency (Oukarroum *et al.* 2007, 2009) or high salt concentration (Mathur *et al.* 2013, Li *et al.* 2015) can also cause the K-band to appear. The appearance of the K-step during OJIP transient has been proposed as a test for stress conditions (Srivastava *et al*. 1997).

A widespread method for analyzing stress effects on the PSA is the JIP-test developed by Strasser (Strasser and Strasser 1995). The JIP-test allows one to evaluate the efficiency of electron transfer stages using the parameters of the induction curve. This method has been successfully applied for the analysis of effects of macro- and micronutrient deficiency on the functioning of the photosynthetic machinery in tomato and maize plants (Kalaji *et al.* 2014), sulfur deficiency effects on *Raphanus sativus* (Samborska *et al.* 2019), and nitrogen deficiency in *Actinidia arguta* (Swoczyna *et al.* 2019). Solovchenko *et al.* (2013) studied the applicability of OJIP parameters for online monitoring of physiological state and accumulation of lipids in microalgal cultures grown in photobioreactors. Stirbet *et al.* (2018) reviewed how some JIP-test parameters, namely performance indices, PIs, help in the assessment of photosynthetic tolerance to abiotic stresses. All the authors concluded that the JIP-test parameters are suitable markers of stress responses and other important phenotypic traits.

Another method to analyze the fluorescence transients is deconvoluting them into exponentials roughly corresponding to the OJIP phases (Boisvert *et al.* 2006, Antal and Rubin 2008). Changes in the characteristic times and amplitudes of the exponential functions show the dynamics of the OJIP phases. In most of the papers, deconvolution with a predefined number (commonly three) of exponentials is used (Boisvert *et al.* 2006, Antal and Rubin 2008). The method of spectral multiexponential approximation (SMEA) (Plyusnina *et al.* 2015) allows one to estimate a number of exponentials sufficient for a good fitting of the fluorescent transient. Thus, it makes possible to study the dynamics of OJIP phases, tracking their appearance or disappearance, for example, during culture growth. SMEA also allows one to detect visually indistinguishable phases of induction curves. Advent of such phases reflects an increase in the contribution of processes with a characteristic time corresponding to this phase. The SMEA analysis was successfully applied to study the phase dynamics of the OJIP curves in the algae *Chlamydomonas reinhardtii* starving for sulfur (Antal *et al.* 2019), as well as *Chlorella vulgaris* starving for nitrogen (Plyusnina *et al.* 2019). In both cases, additional phases in the OJIP curves associated with stress effects were detected.

In most investigations related to the effects of mineral starvation, the time course of stress onset was studied with rather long intervals, detecting the stress as phenomenon, but overlooking the onset of the stress. More frequent measurements together with an appropriate analysis of large sets of experimental data are needed to identify the processes occurring in the PSA during the stress progress. The construction of photobioreactors (PBRs) with automatic measurement of fluorescence induction curves and absorption spectra from one side (Antal *et al.* 2019, Plyusnina *et al.* 2019), as well as the development of the software package *pyPhotoSyn* that includes above mentioned methods for express analysis of large sets of experimental data (Plyusnina *et al.* 2015), allows us to study such transient processes under stress.

Therefore, the main aim of this study was to perform a detailed analysis by a complex of mathematical methods of the gradual changes in the PSA of the microalgae *Chlorella vulgaris* culture in the PBR under natural depletion of the minerals in the medium. The thermophilic strain with a high growth rate was chosen for detailed documenting of all the stages of the culture growth progressing over a short time (tens of hours). Plyusnina *et al.* (2019) showed that nitrogen depletion in the medium is the limiting factor triggering changes in the PSA during *Chlorella* growth on Tamiya medium (Tamiya 1957). Therefore, we intended to compare the dynamics of the OJIP-curve parameters during the culture growth and the changes of the nitrate content in the medium. We assumed that a complex analysis of gradual changes in the PSA, together with measurements of nitrogen content in the medium and chlorophyll content in cells, would allow us to identify the turning points of metabolic reprogramming during the natural depletion of nitrogen and the onset of nutrient stress.

Materials and methods

Microalgae cultivation: The experiments were performed on batch cultures of the fast-growing thermophilic strain of *Chlorella vulgaris*. Microalgae were cultivated in a 1-L panel PBR made in-house at Biophysics Department of the Lomonosov Moscow State University. The Tamiya medium (Tamiya 1957, Kuznetsov and Vladimirova 1964) diluted at 1:30 was used. The initial pH level was set to 6. The initial optical density of the culture in the PBR was 0.01 per 1 cm at 675 nm. The PBR was continuously illuminated with a LED panel (a warm white LED series) at 180 μmol(photon) m^{-2} s^{-1}. The temperature within the PBR was maintained at 36.0 ± 0.5°C. A CO_2-rich (0.4% CO_2) air mixture was passed through the PBR. The air flow rate was 1 L min^{-1}. The culture was grown in the

PBR for 60 h. Three repetitions (independent 60-h runs in the PBR) of the experiment were performed. The stock culture (inoculum) was grown in constantly rotating flask in the Tamiya medium diluted 1:10 under continuous light illumination with a filament lamp (light intensity of 200 μmol(photon) m^{-2} s^{-1}) and constant temperature (36°C) for 1 d and then transferred into the PBR.

Absorption spectra and chlorophyll (Chl) fluorescence: The absorption spectra of the cell suspension and the Chl fluorescence induction curves were recorded repeatedly during the growth of the algae cell culture. All measurements were performed every hour with an automated instrument (Fig. 1), which consisted of a sample collection unit, an optic module (fluorometer + spectrophotometer), and a personal computer. During each cycle of measurements with the instrument, a sample was pumped from the PBR with the peristaltic pump into the 2-mm optic path length flow cell of the optic module. The pump was stopped for the measurement period. Absorption spectra were measured using a *USB2000+* spectrometer (*Ocean Optics Inc*., USA) with a halogen lamp as a light source. Optical density of the cell suspension at 725 nm was used as cell count index (A_{725}), and the Chl content index was estimated as a difference between optical densities at 675 and 725 nm ($A_{675} - A_{725}$) to account for light scattering. Fluorescence transients were recorded after 3 min of dark adaption. Chl *a* fluorescence was excited at 455 nm [3,000 μmol(photon) m^{-2} s^{-1}] and measured in a region of 670–750 nm with a silicon photodiode *BPW34* (*Vishay Intertechnology Inc*., USA) with 5-mm *PS-8* and *KS-17* colored glass filters (*GOST 94-11-91*, USSR). Within the initial phase of intensive light illumination (0–10 ms) fluorescence intensity was sampled with 10-μs intervals. Further, the 1-ms sampling intervals were applied (10 ms–2 s of fluorescence transient). The spectrophotometer and fluorometer units shared the same photometric flow cell. After the measurement, the sample was pumped back to the PBR, and the transfer tubes and the photometric cell were washed with water.

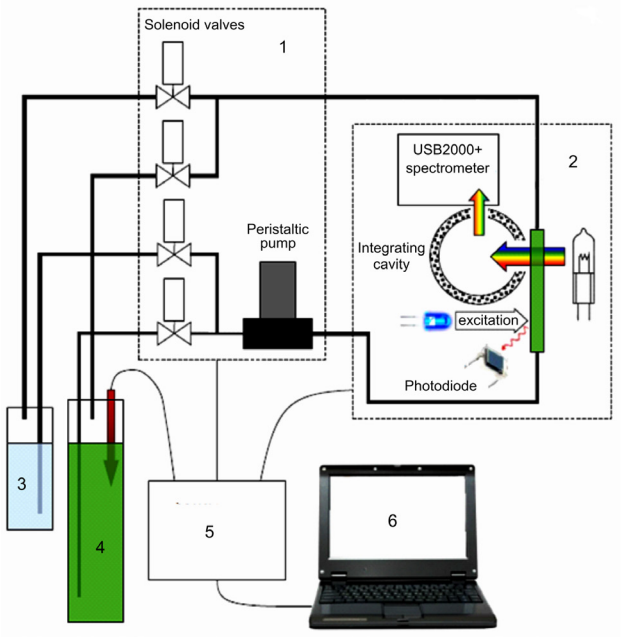

Fig. 1. Experimental setup for automatic measurement of the absorption spectra and chlorophyll fluorescence. 1 – sampler unit, 2 – optic module (fluorometer + spectrophotometer), 3 – tank with water, 4 – photobioreactor (PBR), 5 – controller unit, 6 – personal computer.

Cell counting and determination of nitrogen and Chl contents: During one of the repetitions of the experiment samples were collected for cell counting and for the determination of residual nitrate content in the medium as well as for Chl *a* and *b* assessment in cells. Samples were collected every hour in the period from 20 to 41 h of culture growth synchronously with the absorbance and fluorescence measurements. Cell density of the suspension was determined using a *Multisizer 3* particle analyzer (*Beckman-Coulter*, USA). For nitrogen and chlorophyll content determination, the cells were pelleted by centrifugation at 3,000 × *g* for 3 min. The nitrate content in the supernatant was determined by ion-exchange HPLC using an *ICS 1600* chromatograph (*Thermo Scientific*, USA). To calculate the per-cell nitrogen content, we subtracted nitrate content in the supernatant from its content in the fresh media and divided by the number of cells in the sample. To smooth the experimental noise in cell counting, approximation of cell count with an exponential function was used for calculation of per-cell nitrogen and Chl content. Pigment content was determined spectrophotometrically (*Agilent Cary 300*, *Agilent*, USA) in DMSO extracts of the cells as described previously (Solovchenko *et al.* 2010).

Analysis of fluorescence transients: We used the *pyPhotoSyn* software (Plyusnina *et al.* 2015) to analyze the fluorescence rise kinetics. This software allows calculation of JIP-test parameters for individual fluorescence transients, and calculation of difference curves of normalized variable fluorescence for several transients according to Strasser *et al.* (2004). In addition, this software implements the spectral multiexponential approximation (SMEA) method introduced in Plyusnina *et al.* (2015), which allows to estimate the number of phases of the OJIP curve, their characteristic times and magnitudes. For the list of JIP-test parameters extracted from the recorded fluorescence transients and calculated according to Strasser *et al.* (2004), *see* Appendix. Minimal fluorescence F_0 and initial slope of the fluorescence transient M_0 were estimated as the intercept and the slope of linear approximation of the initial linear segment of the fluorescence transient according to Plyusnina *et al.* (2015).

The spectral multiexponential approximation (SMEA) was performed with the *pyPhotoSyn* software to detect changes in the number of distinguishable OJIP phases and estimate the lifetimes and the magnitudes of the phases (O–J, J–I, I–P phases). Fluorescence transients were approximated by a sum of exponential functions with fixed

characteristic times:

$$F(t) = F_0 + \sum_{n=1}^{N} A_n\left(1 - e^{-t/\tau_n}\right)$$

where A_n is an amplitude of the n-th exponent with characteristic time τ_n. The characteristic times of the exponential functions were selected in a logarithmic grid with a fixed step: $\tau_{n+1} = 1.1\ \tau_n$. The result of the approximation of the input data is presented as a set of amplitudes A_n, corresponding to the selected fixed time τ_n. Summation of the amplitudes A_n at each step of the grid results in a step function:

$$\sum_{i=1}^{n} A_i$$

Thus, SMEA transforms the original OJIP curve with implicit phases to the step-like curve with well-defined phases. The number of steps defines the minimum number of exponential functions which constitute the original curve. Each step represents the yield of the corresponding exponent, its amplitude and lifetime. This step-like curve can be depicted by a color bar, in which height and color (shade of gray) of each band refers to the magnitude and lifetime of the corresponding kinetic phase of the OJIP curve (Fig. 2). SMEA transforms of multiple fluorescence transients may be plotted together as a single heat map, providing a pictorial representation of gradual changes in the phases of all OJIP curves recorded during the microalgae growth. The details of the SMEA are provided in Plyusnina *et al.* (2015, 2019).

Results

Cell division rate and nitrogen and Chl content: During the first 40 h of *Chlorella* culture growth in the PBR, the cell count revealed the exponential dependence on time, and satisfied the equation $y = 1.5 \cdot e^{0.08 \cdot t}$ (Fig. 3*A*, *black diamonds* and *dashed curve*, respectively). Thus, cell doubling time on the exponential phase of culture growth may be estimated as 9 h. For this period, the cell count had a good fit to the cell count index A_{725} obtained from light absorption measurements (Fig. 3*A*, *white circles*).

The change in the total Chl content in the culture (Fig. 3*B*, *black diamonds*) coincided with the change of Chl content index $A_{675} - A_{725}$ (Fig. 3*B*, *white circles*) until 30 h of the culture growth. Then, the total Chl content stopped increasing, while $A_{675} - A_{725}$ continued increasing. We believe that it was due to so-called packaging effect: the same amount of Chl leads to a higher absorption when the molecules of the pigment are packed more loosely. Likely, it was the case under our experimental conditions since the number of cells increased and the amount of Chl remained the same.

The initial concentration of KNO_3 in the cultivation medium before *Chlorella* inoculation was 52 mg L^{-1}. It decreased with the culture growth and approached its steady-state value (0.7 mg L^{-1}) within 31 h (Fig. 3*C*). During the exponential growth phase, the per-cell nitrogen and Chl contents (Fig. 3*D*, *white circles* and *black diamonds*, respectively) remained almost constant, and started decreasing when nitrate was depleted in the medium, as the cells continued dividing and their number was increasing. Per-cell nitrogen and Chl content decreased almost three times until 41 h of cultivation. It should be noted that the Chl content per cell decreased with the same rate as the nitrogen content.

Assessing functional activity of the photosynthetic apparatus by JIP-test: Prompt Chl fluorescence rise kinetic curves were recorded every hour during the 60 h of *Chlorella* cultivation in the PBR. Using *pyPhotoSyn* software, we analyzed the gradual changes in the JIP-test parameters. Here, we showed the data in range from 20–50 h of the experiment, where we got reliable

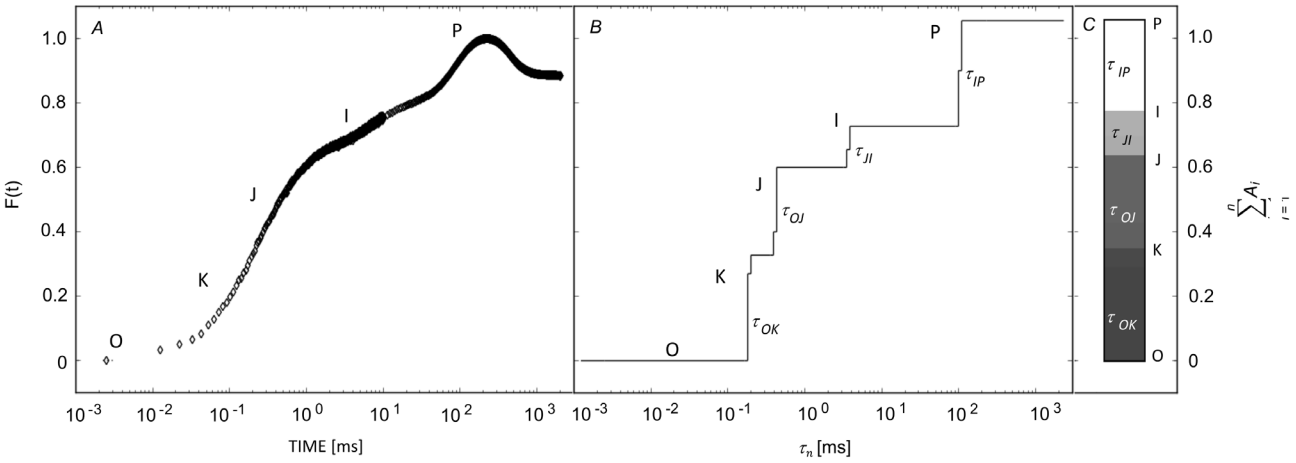

Fig. 2. SMEA transformation of the fluorescence transient. (*A*) Normalized variable fluorescence transient (experimental data) with obscured phases. (*B*) Step function obtained by SMEA transform. (*C*) Color bar representation of SMEA transform with shades of grey representing different characteristic times of exponential functions corresponding to the phases of the fluorescence rise. Letters OKJIP denote detected phases of the fluorescence rise.

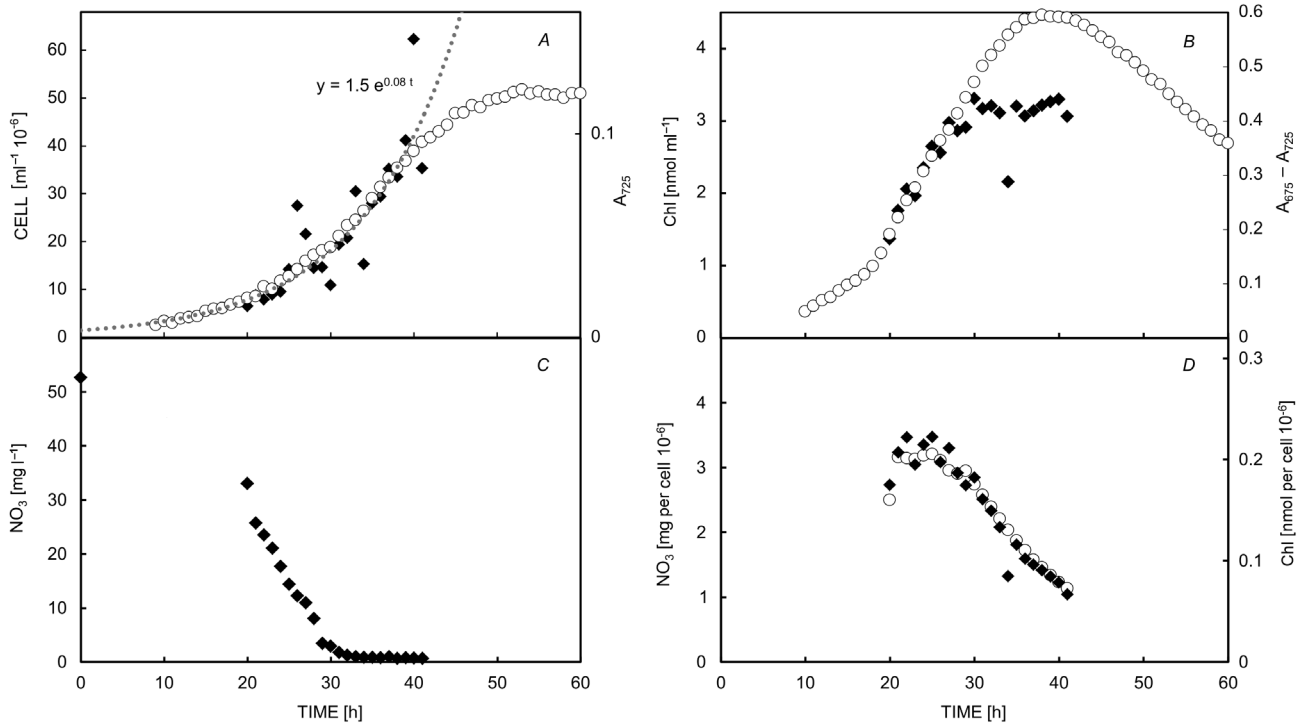

Fig. 3. Cell density, chlorophyll, and nitrogen content changes during *Chlorella* growth in the photobioreactor. (*A*) Cell count (*black diamond*), its approximation by the exponential function $y = 1.5 \cdot e^{0.08 \cdot t}$ (*dashed curve*) and cell count index estimated as optical density of the cell suspension at 725 nm (A_{725}, *white circles*). (*B*) Total content of chlorophyll *a* and *b* (*black diamond*) and its estimation (chlorophyll content index) by the optical density of the cell suspension A_{675} corrected to light scattering ($A_{675} - A_{725}$, *white circles*). (*C*) Nitrate content in the medium. (*D*) Per-cell nitrogen (*white circles*) and chlorophyll *a* and *b* (*black diamond*) content.

estimations of all the parameters. Out of this range the fluorescence transients were too noisy: due to very low cell density during the first 20 h of the culture growth, and due to low variable fluorescence after 50 h.

The maximal quantum yield of PSII photochemistry $\varphi_{Po} = F_v/F_m$ was almost constant (0.67) up to 35 h of the culture growth, and then declined slowly to about 0.6 (at 42 h) and less (Fig. 4*A*). Relative variable fluorescence at the J-step V_J increased gradually up to 29 h, then dropped sharply within 3 h, and started to increase again (Fig. 4*B*). The performance index PI_{ABS} (Fig. 4*C*) reached its maximum (0.7) at 20 h of culture growth (the first time point when reliable determination of JIP-test parameters became possible), then gradually decreased to about 0.3 at 29 h and further increased to 0.4 at 31 h, then declined monotonously to 0.2 at 45 h and later. The plots of the initial slope of the fluorescence transient M_0 (Fig. 4*D*), normalized complementary area above the O-J-I-P transient S_m (Fig. 4*E*), and quantum yield of electron transport φ_{E0} (Fig. 4*F*) also displayed two inflections (at 29 and 32 h of culture growth).

Thus, we found two moments of time where time course of most JIP-test parameters sharply changed during *Chlorella* cultivation – 29 and 32 h. However, using these parameters to calculate energy fluxes per RC: trapped energy flux TR_0/RC (Fig. 4*G*), electron transport flux ET_0/RC (Fig. 4*H*), and dissipated energy flux DI_0/RC (Fig. 4*I*), one can find that each of them changed at a single time point, although the expressions for all fluxes contained the parameter V_J with two inflection points (Fig. 4*B*). The rate of electron transport ET_0/RC increase changed sharply at 29 h, whereas the rates of increase of both trapped TR_0/RC and dissipated energy fluxes DI_0/RC changed at 32 h. The described abrupt changes were clearly visible on a large scale, and not so well on a small scale, however, the repeatability in the three experiments confirmed that these changes were significant.

Assessing PSII donor side activity by fluorescence transients difference: Comparison of fluorescence transients by subtraction of one double-normalized curve from another one is helpful for detecting changes in the initial part of the OJIP curve, in particular, the appearance of the K-band. To reveal the dynamics of K-step during the culture growth, we plotted fluorescence transients double normalized to O–J phase as $W_{OJ} = (F_t - F_0)/(F_J - F_0)$ (Fig. 5*A*) as described in Oukarroum *et al.* (2007). The averaged fluorescence transient for the three repetitions of the experiment recorded at 23 h of the culture growth in the PBR was taken as a reference curve. By this time, the density of the culture had grown sufficiently so the fluorescence transients were recorded with minimal noise, while the culture had not yet gone to starve since there was a sufficient amount of nitrogen remained in the medium. The differences ΔW_{OJ} were constructed by subtracting reference W_{OJ} from W_{OJ} calculated for transients recorded

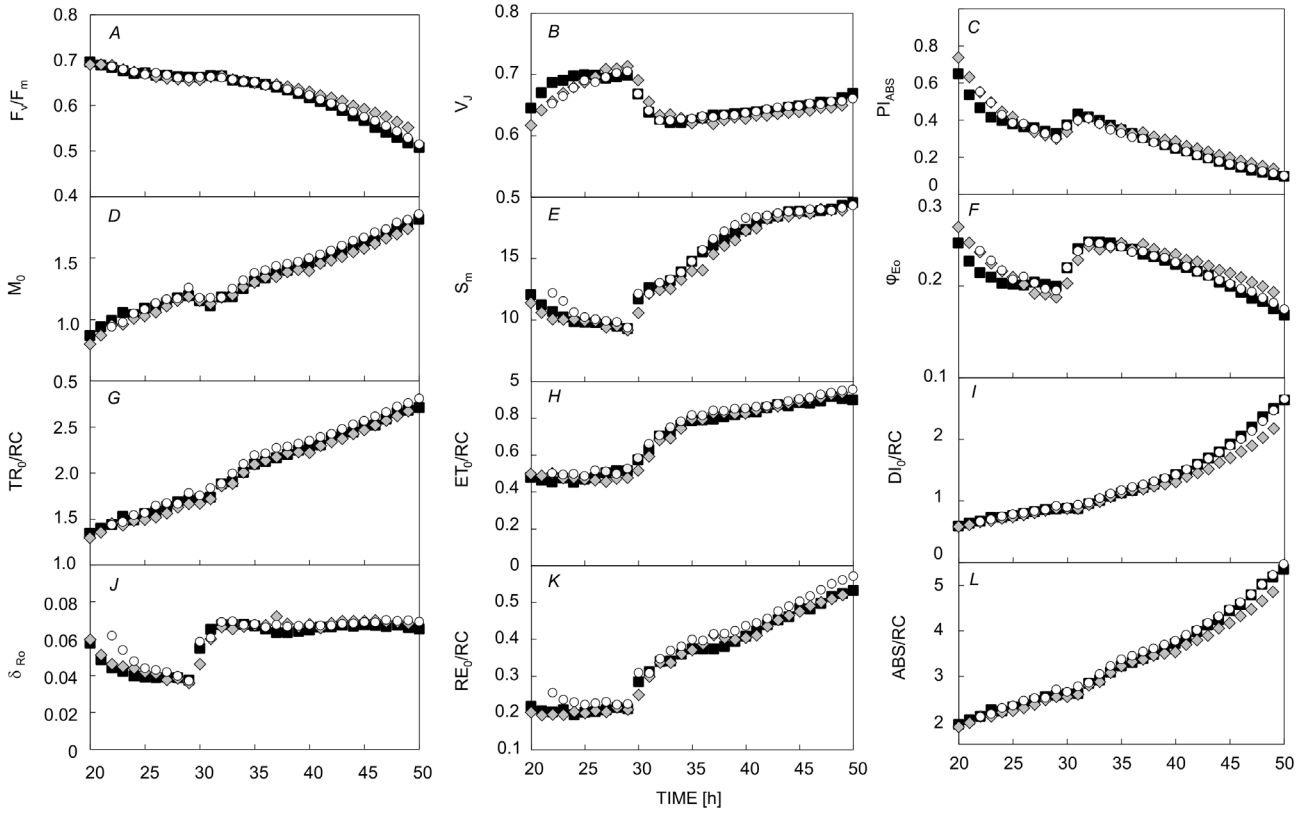

Fig. 4. Dynamics of the JIP-test parameters during the *Chlorella* culture growth in the photobioreactor. Chlorophyll *a* fluorescence transients were recorded after 3 min of dark adaption, excitation lite intensity was 3,000 μmol(photon) m^{-2} s^{-1}. Three repetitions of the experiment are shown with different symbols.

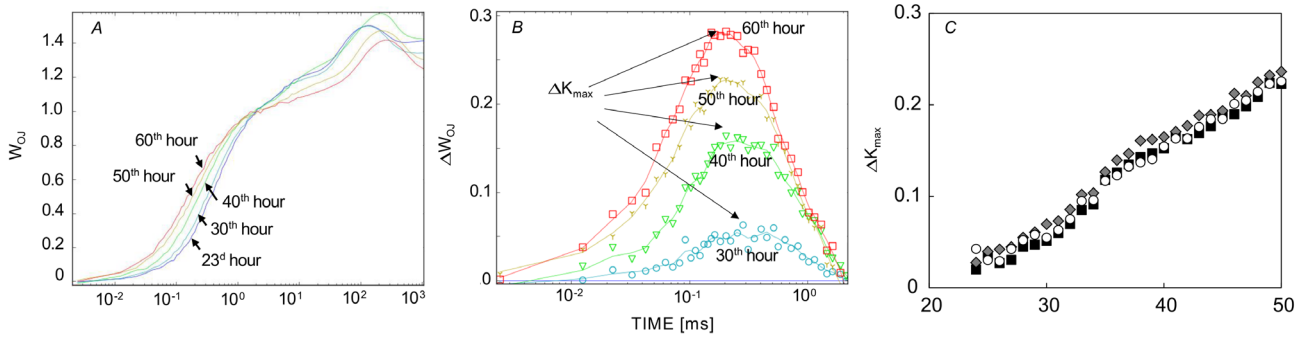

Fig. 5. Estimation of K-band amplitude from fluorescence transients difference. (*A*) Fluorescence transients normalized to OJ phase. $W_{OJ} = (F_t - F_0)/(F_J - F_0)$. (*B*) The difference of fluorescence transients normalized to OJ phase. The averaged fluorescence transient for three repetitions of the experiment recorded at 23 h of the culture growth in the photobioreactor was taken as a reference curve W_{ref}. $\Delta W_{OJ} = W_{OJ} - W_{ref}$. (*C*) ΔK_{max} is the maximal value of corresponding ΔW_{OJ} in the time interval from 0 to 2 ms. The three repetitions are shown with different symbols.

at any subsequent hour of culture growth (Fig. 5*B*). Each of these differences has a maximum (K-peak) at *ca*. 250 μs.

As a rule, in the literature, changes in the K-peak are described only qualitatively, as its increase or decrease. To provide a more convenient way to assess the OEC activity for a large experimental dataset, we introduced a quantitative estimation for the K-peak magnitude. The maximum value of ΔW_{OJ} was designated as ΔK_{max} (Fig. 5*B*). Having determined ΔK_{max} for each hour of culture growth, we could plot its change (Fig. 5*C*) and thus evaluate gradual changes in the OEC activity during microalgae growth. ΔK_{max} increased from the beginning of the observation and had some nonmonotonic changes at 35 h of culture growth.

Refinement of O-J-I-P phases by the SMEA analysis: SMEA analysis showed that during the first 35 h of the cultivation the fluorescence rise can be decomposed to

three exponentials with characteristic times in the ranges 0.4–0.5 ms, 2.6–4.2 ms, and 55–130 ms corresponding to the typical OJ, JI, IP phases. It should be noted here that these characteristic times refer to the moments of time when fluorescence is *e* (*ca*. 2.7) times lower than that in the steady state of the corresponding phase, so these times were significantly smaller than those usually used to describe OJIP curve phases. An additional phase with a characteristic time at *ca*. 250 μs appeared after 35 h of culture growth (Fig. 6). The characteristic time of this additional phase correlates with the time of K-peak detected by subtracting one fluorescence transient from another. The characteristic time of the OJ and OK phases in the multiexponential approximation decreased during the growth of the culture, while the characteristic time of the JI and IP phases increased (Fig. 6).

Discussion

Analysis of the fluorescence transients recorded during the growth of the *Chlorella* culture together with monitoring the residual nitrogen and cell Chl contents showed that the fluorescence transients can serve as a sensitive tool to characterize processes in the PSA that occur when the minerals in the medium are depleted. Almost complete depletion of nitrogen in the medium occurred at 30 h of the culture growth. However, the first symptoms of stress could be detected a few hours earlier. Combining the JIP-test, ΔW_{OJ} differential curves, and SMEA with traditional methods of chemical analysis, we identified several qualitatively different stages in the growth of the *Chlorella* algae batch culture in the PBR: exponential growth, stress acclimation, stressed cells. Three corresponding pivot points of the culture growth can be distinguished in this regard at 29, 32, and 35 h.

During the first stage (up to 29 h), there was still enough nitrogen in medium, so the culture growth was still exponential. At this stage, maximum quantum yield of primary photochemistry, φ_{P0}, remained constant, however, the performance index, PI_{ABS}, decreased due to simultaneous decrease of ψ_0 – the probability that a trapped exciton moves an electron into the electron transport chain beyond Q_A and increase of the effective antenna cross-sectional area ABS/RC. These effects can be explained by the increase of optical density of cell suspension, which causes the average illumination in the PBR to decrease.

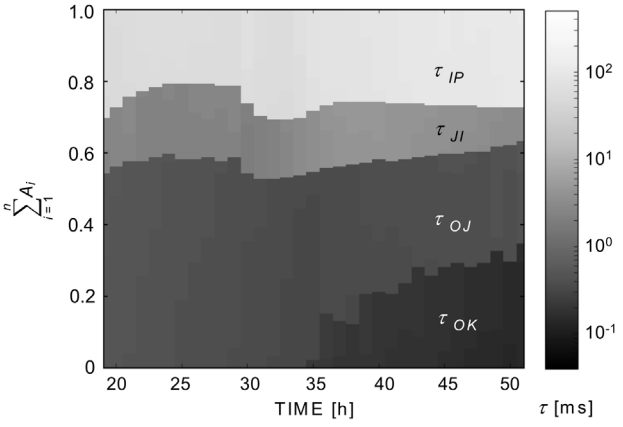

Fig. 6. The amplitudes of the phases of multi-exponential approximation of OJIP curves for every hour of the culture growth in the photobioreactor. *Shades of gray* indicate the characteristic time of the identified phases. τ_{OK} ~ 0.15–0.25 ms, τ_{OJ} ~ 0.4–0.5 ms, τ_{JI} ~ 2.6–4.2 ms, τ_{IP} ~ 55–130 ms.

After 29 h, the consumption of nitrate from the medium by the cells nearly stopped. At the same time, the biosynthesis of Chl also stopped. Nevertheless, cell division continued at the same rate leading to a decrease in the per-cell content of nitrogen and Chl.

Moreover, in the interval from the 29–32 h, there was a noticeable increase in the performance of the PSA PI_{ABS} and in ψ_0. This effect might be explained by the decrease of the PSII RC density in the thylakoid membrane resulting in an increase in the size of plastoquinone pool per RC. This hypothesis was supported by a sharp increase in the area above the induction curve S_m, and in δ_{R0} – the probability of electron transfer from intersystem carriers to PSI. During this period, the effective cross-sectional area of the antenna ABS/RC did not change.

After 32 h of the culture growth, the performance of the PSA, PI_{ABS}, began decreasing again. This decrease was mostly a result of the lowering of the maximum quantum yield of primary photochemistry, φ_{P0}. It is likely that at this stage reparation of the damaged PSII RCs failed due to impairment protein and pigment syntheses under nitrogen depletion. At the same time, the effective antenna cross-sectional area ABS/RC began to increase, also likely due to damage to the PSII RCs resulting in an increase in the number of LHC complexes per each of the remained active PSII RCs. However, the extra light energy trapped by the increased antenna cannot be efficiently utilized by the RCs, so the energy dissipation DI_0/RC also increased.

Nevertheless, in the interval from 29–35 h, electron transport flux ET_0/RC almost doubled, whereas after 35 h, ET_0/RC increased slower. Around this time, the Chl content index ($A_{675} - A_{725}$) reached its maximum and began to decline. At the same moment an additional fast phase (K-band) with a characteristic time of *ca*. 0.25 ms appeared in the SMEA decomposition of the fluorescence transient likely manifesting inhibition of the electron transport on the PSII donor side. We suppose that degradation of the PSA under our experimental conditions began from this moment.

The analysis of difference curves ΔW_{OJ} revealed the appearance of K-peak as well, but its magnitude ΔK_{max} grew from the very beginning of observation when nitrate in the media was not depleted yet. Simultaneously we observed the increase in the effective antenna cross-sectional area, ABS/RC, and trapped energy flux, TR_0/RC. Vredenberg (2008) proposed a model that could explain the appearance of the K-peak by an increase in light trapping due to the increase of the antenna cross section. In line with this reasoning, we assumed that at the initial growth stage the increase of K-peak can be explained by the increase of antenna cross section. At 35 h of the cultivation, one can see a nonmonotonous change in ΔK_{max}. A further increase

in ΔK_{max} may reflect the changes in the PSII donor side activity, that is consistent with the results of the SMEA analysis.

The period from the 29–35 h can be considered as the acclimation period. During this period, the PSA retains the ability to cope with the nutrient starvation. It should be mentioned that the duration of this period (*ca*. 6 h) is shorter than the doubling time at the exponential phase (*ca*. 9 h). Therefore, the increase in the cell number observed at this time is due to division of the cells that committed cell division before the depletion of nitrogen in the medium.

Recording of the OJIP curves for every hour during a large period of microalgae *Chlorella* growth allowed us to reveal the rapid transient response of the PSA to nitrogen depletion. This approach has promise for rapid characterization of different stages of algal cells acclimation to nutrient starvation.

Conclusion: A complex analysis of photosynthetic activity on the background of nitrogen depletion in batch culture of a thermophilic strain of *Chlorella vulgaris* was performed. Three pivot points in the kinetics of the key photosynthetic parameters were detected. A rapid transient rise of the efficiency of PSII was detected immediately after depletion of nitrogen in the medium. During this period, the PSA coped with the stress by (*1*) reducing the density of PSII RCs in the thylakoid membranes and (*2*) by a simultaneous increase in the effective cross section of the light-harvesting antenna, and the cells continued to divide. Further nitrogen starvation led to deactivation of the oxygen-evolving complex and the decline of the overall electron transport.

The JIP-test proved to be a highly sensitive method for detecting gradual changes in microalgae PSA during the onset of nutrient starvation stress. Together with the SMEA and the analysis of differential curves ΔW_{OJ}, the JIP-test can be used to develop a comprehensive approach to the monitoring and control of the photosynthetic activity and stress responses of the photosynthetic cells.

References

Antal T., Konyukhov I., Volgusheva A. *et al.*: A chlorophyll fluorescence induction and relaxation system for the continuous monitoring of photosynthetic capacity in photobioreactors. – Physiol. Plantarum **165**: 476-486, 2019.

Antal T., Rubin A.: *In vivo* analysis of chlorophyll *a* fluorescence induction. – Photosynth Res. **96**: 217-226, 2008.

Boisvert S., Joly D., Carpentier R.: Quantitative analysis of the experimental O-J-I-P chlorophyll fluorescence induction kinetics. Apparent activation energy and origin of each kinetic step. – FEBS J. **273**: 4770-4777, 2006.

Kalaji H.M., Oukarroum A., Alexandrov V. *et al.*: Identification of nutrient deficiency in maize and tomato plants by *in vivo* chlorophyll *a* fluorescence measurements. – Plant Physiol. Bioch. **81**: 16-25, 2014.

Kuznetsov E.D., Vladimirova M.G.: [Iron as a factor limiting the growth of *Chlorella* on Tamiya medium.] – Sov. Plant Physiol. **11**: 82-89, 1964. [In Russian]

Li X.M., Zhang L.H.: Endophytic infection alleviates Pb^{2+} stress effects on photosystem II functioning of *Oryza sativa* leaves. – J. Hazard. Mater. **295**: 79-85, 2015.

Lin Z.H., Chen L.S., Chen R.B. *et al.*: CO_2 assimilation, ribulose-1,5-bisphosphate carboxylase/oxygenase, carbohydrates and photosynthetic electron transport probed by the JIP-test, of tea leaves in response to phosphorus supply. – BMC Plant Biol. **9**: 43, 2009.

Mathur S., Mehta P., Jajoo A.: Effects of dual stress (high salt and high temperature) on the photochemical efficiency of wheat leaves (*Triticum aestivum*). – Physiol. Mol. Biol. Pla. **19**: 179-188, 2013.

Oukarroum A., El Madidi S., Schansker G. *et al.*: Probing the responses of barley cultivars (*Hordeum vulgare* L.) by chlorophyll *a* fluorescence OLKJIP under drought stress and re-watering. – Environ. Exp. Bot. **60**: 438-446, 2007.

Oukarroum A., Schansker G., Strasser R.J.: Drought stress effects on photosystem I content and photosystem II thermotolerance analyzed using Chl *a* fluorescence kinetics in barley varieties differing in their drought tolerance. – Plant Physiol. **137**: 188-199, 2009.

Plyusnina T.Yu., Khruschev S.S., Frolov A.E. *et al.*: Monitoring of the photosynthetic activity of the microalgae *Chlorella* under nitrogen depletion conditions. – Biophysics **64**: 358-366, 2019.

Plyusnina T.Yu, Khruschev S.S., Riznichenko G.Yu., Rubin A.B.: Analysis of chlorophyll fluorescence transient by spectral multi-exponential approximation. – Biophysics **60**: 392-399, 2015.

Samborska I.A., Kalaji H.M., Sieczko L. *et al.*: Can just one-second measurement of chlorophyll *a* fluorescence be used to predict sulphur deficiency in radish (*Raphanus sativus* L. *sativus*) plants? – Curr. Plant. Biol. **19**: 100096, 2019.

Schmidt S.B., Powikrowska M., Krogholm K.S. *et al.*: Photosystem II functionality in barley responds dynamically to changes in leaf manganese status. – Front. Plant Sci. **7**: 1772, 2016.

Solovchenko A., Merzlyak M., Khozin-Goldberg I. *et al.*: Coordinated carotenoid and lipid syntheses induced in *Parietochloris incisa* (Chlorophyta, Trebouxiophyceae) mutant deficient in Δ5 desaturase by nitrogen starvation and high light. – J. Phycol. **46**: 763-772, 2010.

Solovchenko A., Solovchenko O., Khozin-Goldberg I. *et al.*: Probing the effects of high-light stress on pigment and lipid metabolism in nitrogen-starving microalgae by measuring chlorophyll fluorescence transients: Studies with a Δ5 desaturase mutant of *Parietochloris incisa* (Chlorophyta, Trebouxiophyceae). – Algal Res. **2**: 175-182, 2013.

Srivastava A., Guissé B., Greppin H., Strasser R.J.: Regulation of antenna structure and electron transport in photosystem II of *Pisum sativum* under elevated temperature probed by the fast polyphasic chlorophyll *a* fluorescence transient: OKJIP. – BBA-Bioenergetics **1320**: 95-106, 1997.

Stirbet A., Lazár D., Kromdijk J., Govindjee: Chlorophyll *a* fluorescence induction: Can just a one-second measurement be used to quantify abiotic stress responses? – Photosynthetica **56**: 86-104, 2018.

Stirbet A., Riznichenko G.Yu., Rubin A.B., Govindjee: Modeling chlorophyll *a* fluorescence transient: relation to photosynthesis. – Biochemistry-Moscow+ **79**: 291-323, 2014.

Strasser B.: Donor side capacity of Photosystem II probed by chlorophyll *a* fluorescence transients. – Photosynth. Res. **52**: 147-155, 1997.

Strasser B.J., Strasser R.J.: Measuring fast fluorescence transients to address environmental questions: The JIP test. – In: Mathis P. (ed.): Photosynthesis: From Light to Biosphere. Vol. 5. Pp. 977-980. Kluwer Academic Publishers, Dordrecht 1995.

Strasser R.J., Tsimilli-Michael M., Srivastava A.: Analysis of the chlorophyll *a* fluorescence transient. – In: Papageorgiou G.C., Govindjee (ed.): Chlorophyll *a* Fluorescence: A Signature of Photosynthesis. Advances in Photosynthesis and Respiration. Pp. 321-362. Springer, Dordrecht 2004.

Swoczyna T., Lata B., Stasiak A. *et al*: JIP-test in assessing sensitivity to nitrogen deficiency in two cultivars of *Actinidia arguta* (Siebold et Zucc.) Planch. ex Miq. – Photosynthetica **57**: 646-658, 2019.

Tamiya H.: Mass culture of algae. – Ann. Rev. Plant Physio. **8**: 309-334, 1957.

Vredenberg W.J.: Analysis of initial chlorophyll fluorescence induction kinetics in chloroplasts in terms of rate constants of donor side quenching release and electron trapping in photosystem II. – Photosynth. Res. **96**: 83-97, 2008.

Appendix. JIP-test parameters calculated according to Strasser *et al.* (2004):

F_0 – minimal fluorescence, when all PS II RCs are open
$F_K = F_{300\mu s}$ – fluorescence level at the K-step (300 μs) of the transient
$F_J = F_{2ms}$ – fluorescence level at the J-step (2 ms) of the transient
$F_I = F_{30ms}$ – fluorescence level at the I-step (30 ms) of the transient
F_P (= F_m) – maximal recorded fluorescence, at the peak P of the transient
$F_v = F_m - F_0$ – maximal variable fluorescence
$V_t = (F_t - F_0)/(F_m - F_0)$ – relative variable fluorescence at time t
$V_J = (F_J - F_0)/(F_m - F_0)$ – relative variable fluorescence at the J-step
M_0 – approximated initial slope (in ms^{-1}) of the fluorescence transient V_t
$\varphi_{P0} = F_v/F_m$ – maximum quantum yield of primary photochemistry (at t = 0)
$\psi_0 = 1 - V_J$ – probability (at t = 0) that a trapped exciton moves an electron into the electron transport chain beyond Q_A
$\varphi_{E0} = ET_0/ABS = (1 - F_0/F_m)\ \psi_0$ – quantum yield of electron transport (at t = 0)
$\delta_{R0} = (1 - V_J)\ (1 - V_I)$ – probability with which an electron from the intersystem electron carriers moves to reduce end electron acceptors at the PSI acceptor side
S_m = (Area)/($F_m - F_0$) – normalized total complementary area above the O-J-I-P transient (reflecting multiple-turnover Q_A reduction events)
$ABS/RC = M_0\ (1/V_J)\ (l/\varphi_{P0})$ – absorbed light flux per PSII RC
$TR_0/RC = M_0\ (1/V_J)$ – trapped energy flux further than Q_A^- per PSII RC (at t = 0)
$ET_0/RC = M_0\ (1/V_J)\ \psi_0$ – electron transport flux per PSII RC (at t = 0)
$DI_0/RC = (ABS/RC) - (TR_0/RC)$ – dissipated energy flux per PSII RC (at t = 0)
$RE_0/RC = M_0\ (1/V_J)\ (1 - V_I)$ – electron flux reducing end electron acceptors at the PSI acceptor side per PSII RC
$PI_{ABS} = (RC/ABS)\ [\varphi_{P0}\ (1 - \varphi_{P0})^{-1}]\ [\psi_0\ (1 - \psi_0)^{-1}]$ – performance index on absorption basis